ASM Sc. J., 20(2), 2025
https://doi.org/10.32802/asmscj.2025.1774

Utilisation of Raw Marsh Clam Shell as Adsorbent for Phosphate Removal via Different Concentration of Aqueous Solution

N. A. Hassan[1]*, N. H. Muslim[1], N.H. Abdullah[2]*, H.Y. Chong[1], K.L. Tan[2], O.T. Lee[2], W.P. Low[3], and N.S.A. Zainal[4]

[1]*Faculty of Engineering Technology, Universiti Tun Hussein Onn Malaysia, Hab Pendidikan Tinggi Pagoh, KM 1, Jalan Panchor, 84600 Muar, Johor, Malaysia*

[2]*Neo Environmental Technology, Centre for Diploma Studies, Universiti Tun Hussein Onn Malaysia, Pagoh Education Hub, 84600 Pagoh, Johor, Malaysia*

[3]*Faculty of Engineering and Quantity Surveying, Inti International University, Nilai 71800, Negeri Sembilan, Malaysia*

[4]*Multi Tank Terminal Sdn Bhd, PT 64374, Jalan Perigi Nenas 8/8, Taman Perindustrian Pulau Indah, Pulau Indah, Westport, 42920 Pelabuhan Klang, Selangor*

Nutrient pollution is one of the most challenging environmental problems worldwide. Excess phosphate in water causes eutrophication, where algae bloom occurs and deteriorates water quality due to decreasing oxygen levels, affecting aquatic life. Marsh clam shell has potential as an adsorbent material due to its plentiful supply and good absorption capability towards phosphate. The aim of this study is to investigate phosphate removal by using raw marsh clam shell as the adsorbent in different concentrations of aqueous solution (5, 10, 15, 20, and 25 mg/L) in batch experiments. The mass of adsorbent was kept constant at 2 g and the volume of aqueous solution was fixed at 100 mL. Phosphate removal for the solution with 25 mg/L concentration was the highest, 5.8% compared to other concentrations. The experimental data obtained were compared to the theoretical data. The experimental data fitted well with the pseudo-second-order kinetic model (R^2 = 1) and Freundlich isotherm model (R^2 = 0.9982), suggesting that phosphate adsorption onto raw marsh clam shell is a chemical and multilayer sorption. In conclusion, the application of raw marsh clam shells for phosphate removal from aqueous solutions has potential as a low-cost and effective future wastewater treatment alternative for domestic and industrial wastewater treatment systems.

Keywords: phosphate; marsh clam shell; adsorption; pseudo-second-order kinetics; Freundlich isotherm

I. INTRODUCTION

Water is one of the basic needs that are required by all life on earth. It dominates a majority of spaces in our planet, covering about 71% of the total surface area of the earth (Senthil *et al.,* 2019). However, water as a medium for waste transport is easily contaminated by human activities (Schweitzer *et al.,* 2018). Nowadays, wastewater problems have become one of the global issues of concern as it involves all the lives on this planet. Wastewater that is left untreated before discharge will lead to many problems; for example, it will cause aquatic plants or animals' death due to pollution (Hairom *et al.,* 2021). One of the main reasons for deteriorating water quality is eutrophication. More than 60% of the 90 main lakes in Malaysia have been eutrophicated (Rashid *et al.,* 2020). One of the nutrients contributing to this environmental pollution is phosphate. Phosphate is commonly found in organic wastes from agriculture, sewage, industrial effluent, and manure. It is an

*Corresponding author's e-mail: noorul@uthm.edu.my

important element for plant life; yet excess phosphate is hazardous to the environment.

Fertiliser usage is one of the reasons of eutrophication because fertilisers contain large amounts of phosphate. Fertilisers may boost plant growth, but they will also cause excessive growth for aquatic plants due to the enrichment of nutrients when the phosphates flow into lakes or rivers. This situation may lead to algae bloom, which is excessive growth of algae. The algae eventually cover the water surface and block the sunlight. In time, aquatic plants will not be able to carry out photosynthesis and die. The food chain will be affected as aquatic animals lose their food source and the amount of dissolved oxygen is reduced (Wang *et al.,* 2021). Besides the usage of fertilisers, detergents and dish soap water are also common sources of water pollution from domestic activities. This is because soap water contains phosphate that may also lead to the same problem previously stated (Koohsaryan *et al.,* 2020). Apart from that, untreated sewage released to water bodies in the environment can destroy aquatic life due to the increase of toxins in the water bodies (Sharma *et al.,* 2021).

Calcium carbonate ($CaCO_3$) can adsorb phosphate in wastewater (Dong *et al.,* 2022). Many natural sources contain $CaCO_3$ such as mussel shells, snail shells, and marsh clam shells. Even though calcium carbonate is recognised as one of the efficient phosphate binders in the phosphate removal process (Kasim *et al.,* 2020), the phosphate adsorption performance using raw marsh clam shell still requires further investigation through kinetic and isotherm models. The objectives of this study are to determine the removal efficiency of phosphate using various concentrations of aqueous solution and verify the experimental and theoretical batch data using kinetic and isotherm model.

II. MATERIALS AND METHOD

A. Preparation of Adsorbent

In this research, raw marsh clam shells (*Polymesoda expansa*) were prepared as adsorbents for phosphate removal and tested using different concentrations of aqueous solution. The marsh clam shells were collected from Bachok, Kelantan, Malaysia. The shells were cleaned by using tap water to remove dirt and contaminants. The shells were then rinsed by using deionised water, dried under the sun, and later left in the oven at 30 °C for 2 days. The raw marsh clam shells were crushed using mortar stone and mixer grinder and subsequently sieved for a size range of 1.18–2.36 mm.

B. Preparation of Aqueous Solution

Potassium dihydrogen phosphate (KH_2PO_4) was used to make an aqueous phosphate solution (Zhang *et al.,* 2020). An amount of 0.1433 g of KH_2PO_4 was added to 1 L of deionised water and dissolved in a volumetric flask to a concentration of 100 mg/L. Then, the 100 mg/L solution was diluted by adding different volumes of deionised water to obtain the desired concentrations, which were 5, 10, 15, 20, and 25 mg/L.

C. Analytical Method

A UV–Vis spectrophotometer (HACH DR 6000) was used to examine phosphate concentration in the aqueous solutions before and after the batch tests by using the amino acid method 8178 with the amino acid reagent solution and molybdate reagent. The physical and chemical characteristics of marsh clam shell were also analysed. The adsorbent was characterised by scanning electron microscopy (SEM) and energy dispersive X-ray fluorescence (EDXRF) (COXEM EM-30AX PLUS SEM) to determine the surface morphology of the membrane. The elemental composition and spectral peaks of the shell were determined using EDXRF analysis in which the characteristic X-rays of elements are separated into a complete fluorescence energy spectrum which is then processed for qualitative or quantitative analysis (Dehvari *et al.,* 2020). For the identification of chemical composition of marsh clam shell, Fourier transform infrared spectroscopy (FTIR) and X-ray diffraction (XRD) analysis were carried out by using Perkin Elmer Spectrum Two FTIR Spectrometer and Second-generation BRUKER D2 Phaser Benchtop XRD, respectively. The FTIR analysis was performed to determine the functional groups of the shell before and after the adsorption process, as the infrared spectrum of the adsorbent was obtained through the infrared radiation (IR) to the material (Zhang *et al.,* 2017). In addition, the

crystallisation or crystal phase composition of the shell was characterised in XRD analysis (Prihanto *et al.,* 2021).

D. Batch Experiment

The effect of various concentrations of aqueous solution on the efficiency of phosphate removal was investigated in this study, where the concentrations were 5, 10, 15, 20, and 25 mg/L. The mass of adsorbent at 2 g with a particle size of 1.18–2.36 mm, as well as 100 mL volume of solution were kept constant. The mixture of phosphate solution and adsorbent was shaken on an orbital shaker at 170 rpm with time intervals of 30, 60, 120, 180, 300, 420, 1860, 3300, and 4740, and 6180 min for 5, 10, 15, 20, and 25 mg/L solutions, as shown in Table 1. Then, a sample was taken and filtered by using a vacuum pump and analysed to determine the final phosphate concentration.

Table 1. Adsorption of phosphate

Time (min)	30, 60, 120, 180, 300, 420, 1860, 3300, 4740, 6180
Adsorbent (g)	2
Volume of KH_2PO_4 (mL)	100
Concentration of aqueous solution (mg/L)	5, 10, 15, 20, 25

E. Adsorption Kinetics Study

In this study, the adsorption kinetics of phosphate from aqueous solution was modelled using pseudo-first-order and pseudo-second-order kinetic models (Kończyk *et al,* 2022). The pseudo-first-order (PFO) model equation is usually applied to represent the adsorption in a liquid–solid system (Steigerwald *et al.,* 2021). It proves that the amount of adsorbate intake is directly proportional to the difference in the concentration. In the pseudo-first-order model, the amount of employed active sites is proportional to the amount of unemployed active sites. There are many models for the removal of various adsorbates that have been conducted, yet it is still necessary to validate their applicability and consistency in their linear and nonlinear forms. The equations of PFO are expressed in Table 2.

Table 2. Differential and linearised forms of PFO equation

Differential form	Linearised form
$\frac{dq_t}{dt} = k_1(q_e - q_t)$	$ln\,(q_e - q_t) = ln\,q_e - k_1 t$

where q_e represents the amount of adsorption when it achieves equilibrium, qt is the amount of adsorption at a certain time (Qu *et al.,* 2022), k_1 indicates the first-order model constant (min^{-1}), which is the speed in achieving the adsorption equilibrium (Mohammed *et al.,* 2019). The linearised equation is matched with the kinetic data to determine the values of q_e and k_1 (El-Khaiary *et al.,* 2010).

Chemisorption is represented by the pseudo-second-order model (PSO). By forming a covalent chemical connection with the adsorbent surface, the adsorbate interacts with it. PSO is frequently used to analyse the adsorption process (Gong *et al.,* 2022). The PSO model is utilised in much research works to forecast the experimental results for adsorption and obtain adsorption rate constants. PSO also estimates that the rate of removal of adsorbent is proportional to the vacant active sites on the adsorbent (Solangi *et al.,* 2021). Therefore, the adsorption rate is manipulated by the amount of adsorbate on the surface of the adsorbent is proportional to the amount of vacant active sites on the adsorbent. The initial solute adsorbed, and the adsorption capacity of the adsorbent can be fitted to this model. The equations of PSO are stated in Table 3.

Table 3. Differential and linearised forms of PSO equation

Differential form	Linearised form
$\frac{dq_t}{dt} = k_2(q_e - q_t)^2$	$\frac{t}{q_t} = \frac{1}{k_2 q_e^2} + \frac{1}{q_e}$

F. Adsorption Isotherms Study

Adsorption isotherms is an empirical relationship between the amount of solute adsorbed by a unit weight of adsorbent and the amount of adsorbate retained in solution at equilibrium. Adsorption performance is commonly described through isotherms that reveal the amount of adsorbate present on the adsorbent. In this study, Langmuir and Freundlich isotherm models were applied to analyse the adsorption systems at equilibrium conditions under various concentrations of aqueous solution (Khamwichit *et al.,* 2022). The adsorption models can be solved by linearisation

where the linear correlation coefficient is indicative of model fittingness because the closest value to the unity provides the best fit (Al-Ghouti *et al.,* 2020). Therefore, the data from the batch experiment for the phosphate removal efficiency were fitted to the Langmuir and Freundlich isotherm models to find the model with the best fit.

The Langmuir isotherm assumes monolayer adsorption onto a surface containing a limited number of adsorption sites of uniform strategies with no transmigration of adsorbate in the plane surface, so no further sorption process will take place at that site once it is filled (Alabbad *et al.,* 2021). This is when the surface reaches a saturation point, and the maximum adsorption of the surface has occurred. Meanwhile, the Freundlich isotherm assumes multilayer adsorption with non-uniform distribution of adsorption heat over the heterogeneous surface, so it defines the surface heterogeneity and the exponential distribution of active sites and their energies (Woo *et al.,* 2022). The parameters from these two isotherm models can be solved in the linear form to determine the best fit data combination even though nonlinear forms of the equations are also suitable for both models. The linear form of the isotherm models is expressed in Table 4.

Table 4. Linear form of adsorption isotherm models

Isotherm models	Linear form	Plot	Parameter
Langmuir	$\frac{1}{q_e} = \frac{1}{K_L q_{max} C_e} + \frac{1}{q_{max}}$	$\frac{1}{q_e}$ vs $\frac{1}{C_e}$	q_{max} (mg g^{-1}) K_L (mg g^{-1}) R^2
Freundlich	$\ln q_e = \ln K_F + \frac{1}{n} \ln C_e$	$ln(q_e)$ vs $\ln(C_e)$	K_F (mg g^{-1}) $\frac{1}{n}$ R^2

where,
q_e: Quantity of adsorbate per the quantity of adsorbent at the equilibrium state (mg/g)
q_{max}: Maximum adsorption capacity (mg/g)
C_e: Equilibrium aqueous concentration of the solute (mg/L)
$\frac{1}{n}$: Adsorption rate
K_F: Freundlich constant
K_L: Langmuir constant

III. RESULT AND DISCUSSION

The marsh clam shell samples before and after the adsorption process were investigated and compared in terms its characteristics and performance. For the physicochemical characterisation of the raw marsh clam shell, SEM–EDXRF and XRD analysis were employed. Furthermore, the batch experiment was conducted to study the removal efficiency and the adsorption capacity of phosphate onto raw marsh clam shell in the aqueous solutions. Lastly, the experimental data were fitted to kinetic and isotherm models to verify the adsorption mechanism.

A. Physicochemical Characterisation of Adsorbent

1. SEM–EDXRF analysis

A scanning electron microscope (SEM) was used to observe the surface structure of marsh clam shell to determine the porosity and surface morphology of the sample. Energy dispersive X-ray fluorescence (EDXRF) was used to determine the percentage of elemental composition of marsh clam shell. SEM photomicrographs of raw marsh clam shell with 1500×, 5000×, and 10000× magnifications are shown in Figure 1, revealing the crystal shapes on the adsorbent surface. Figure 1 shows the surface that was used to analyse the chemical composition of raw marsh clam shell. As shown in Table 5, the chemical composition of marsh clam shells consists of calcium, oxygen, and carbon, where the element with the highest content (46.05%) is oxygen and the lowest content (13.72%) is carbon. The reason for gold (Au) appearing in this result is that the marsh clam shells were coated with a gold layer before SEM and EDXRF analyses as the gold coating makes the spectra clearer and easier to be observed.

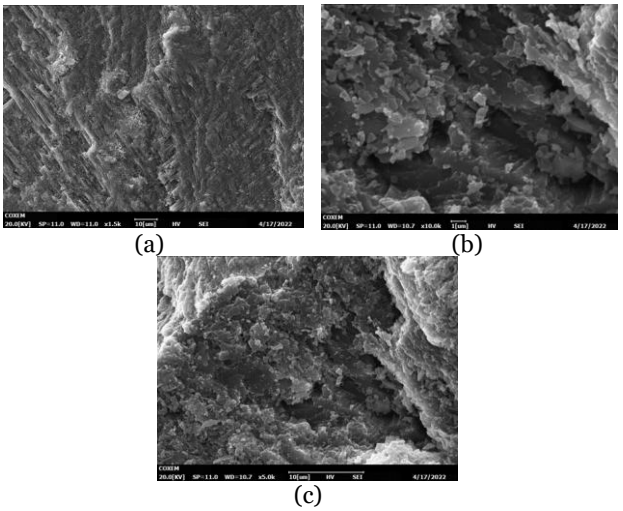

(a) (b)

(c)

Figure 1. SEM images of raw marsh clam shell with (a) 1500×, (b) 5000×, and (c) 10000× magnifications

Table 5. Weight % of elemental composition of raw marsh clam shell from EDXRF spectrum

Element	Ca	O	Au	C
Weight %	34.77	46.05	5.46	13.72

2. FTIR analysis

Fourier transform infrared (FTIR) analysis was performed to identify the chemical functional groups present on the marsh clam shells before and after adsorption. The FTIR spectra were measured in the wavenumber range of 1500–400 cm^{-1} and are shown in Figure 2 and Figure 3. In Figure 2, the peaks before adsorption can be observed at wavenumbers of 1476.54, 862.27, and 712.59 cm^{-1}, representing the existence of CO_3^{2-} in this material (Abou-El-Sherbini *et al.,* 2015). In Figure 3, after adsorption, peaks are observed at 1455.47, 1083.00, 858.94, 712.84, 700.06, and 402.33 cm^{-1} for the carbonate group (Yukhajon *et al.,* 2022). However, the peaks shown in Figure 2 are larger compared to the ones in Figure 3. This is because the number of carbonate group has decreased as some of the carbonate groups have been utilised for the adsorption of phosphate in the aqueous solution (Dodd *et al.,* 2021).

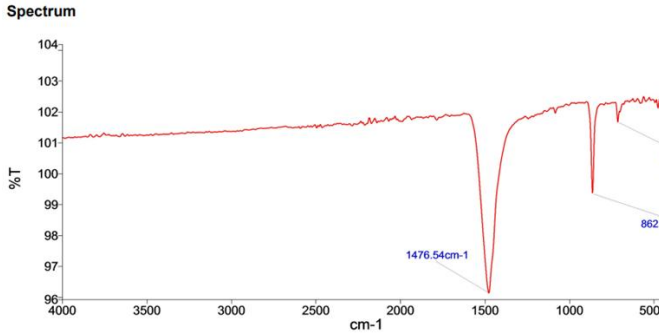

Figure 2. FTIR spectrum of marsh clam shell samples before adsorption

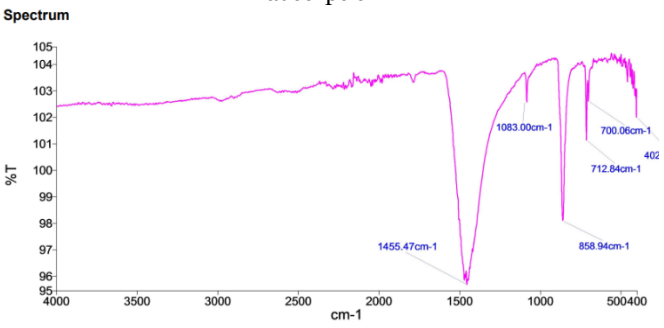

Figure 3. FTIR spectrum of marsh clam shell samples after adsorption

B. Adsorption of Phosphate

The adsorption capacity and removal efficiency were calculated from the experimental data to determine the phosphate adsorption ability of the adsorbent in different initial concentrations of aqueous solution within the time given. In this experiment, the initial concentrations of aqueous solution were set at 5, 10, 15, 20, and 25 mg/L, and each flask was shaken for 10 sets of time. All the data obtained were analysed and the results are presented in Figure 4, Figure 5, and Figure 6. Figure 4 shows that the highest adsorption capacity for the initial concentration of 25 mg/L was 0.071 mg/g, while the highest adsorption capacity for the initial concentration of 5 mg/L was 0.016 mg/g.

Figure 4 shows that the aqueous solution with a high initial concentration resulted in a higher adsorption capacity compared to the solution with the low initial concentration. As for time, the data show that the adsorption capacity of the adsorbent increased with the increase in time. As the time for adsorption increased, the adsorption capacity of the adsorbent in removing the phosphate also increased. Until reaching a certain time, there are no changes of the adsorption capacity due to equilibrium state. It shows that phosphate adsorption has achieved equilibrium, and no more reaction will occur between the adsorbent and phosphate. The increase in the rate of adsorption capacity was high initially and decreased gradually until it reached equilibrium, which is shown by the straight line in the graph where the adsorption capacity remained constant.

The phosphate removal efficiency by marsh clam shell from the aqueous solutions is shown in Figure 5. The solution with 25 mg/L initial concentration showed the highest removal efficiency compared to the other solutions, which was 5.80%. Meanwhile, the lowest removal efficiency (2.15%) was recorded in the solution with 5 mg/L initial concentration. For the other aqueous solutions with concentrations 5, 10, and 15 mg/L, the removal efficiencies were 3.27%, 3.92%, and 5.39%, respectively. In short, a higher maximum removal efficiency was obtained with higher initial concentration. The results obtained from SEM–EDXRF analysis reveal that the adsorbent samples consist of high proportion of calcium (34.77%), which aids in phosphate removal.

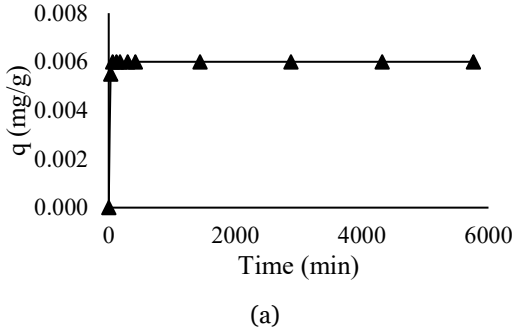

(a)

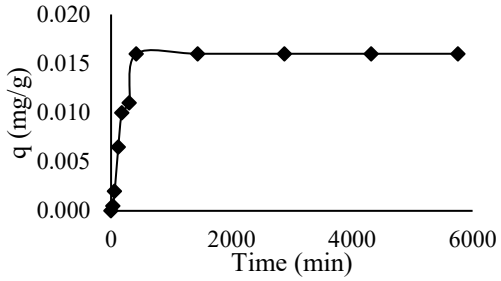

(b)

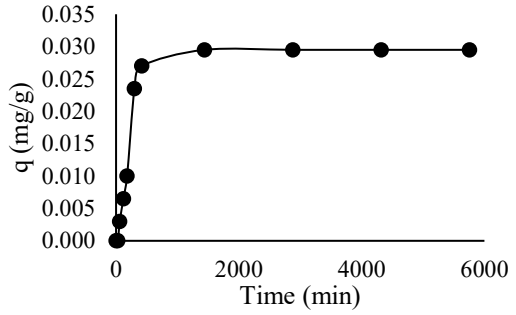

(c)

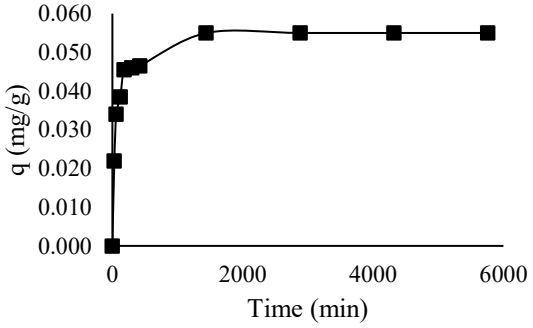

(d)

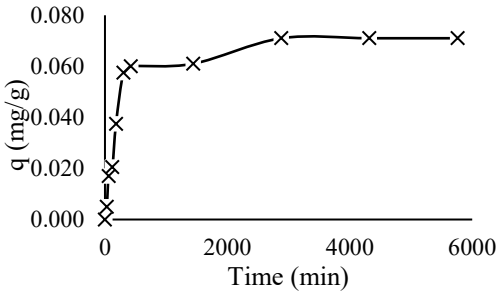

(e)

Figure 4. Adsorption capacity, q (mg/g) for (a) 5, (b) 10, (c) 15, (d) 20, and (e) 25 mg/L solution.

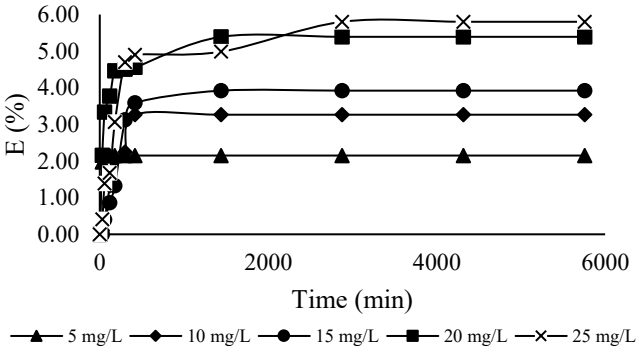

Figure 5. Removal efficiency, E (%) of phosphate from aqueous solution for every concentration

As shown in Figure 6, a graph of removal efficiency (E) and adsorption capacity at equilibrium (q_e) against concentration was plotted to present their relationship. The values of E and qe increased with increasing concentration. The lowest E value was 2.15%, and the lowest qe value was 0.006 mg/g at 5 mg/L of concentration, while the highest E value was 5.8%, and the highest qe value was 0.071 mg/g at 25 mg/L of concentration. This shows that the concentration of aqueous solution is a governing factor influencing the E and q_e values, which are the overall phosphate removal performance of the adsorbent. The increase of uptake capacity corresponding to the increase of phosphate concentration relates to the increase of sorbate quantity that signifies the relatively high solute concentration gradient (Abdel Maksoud *et al.,* 2020).

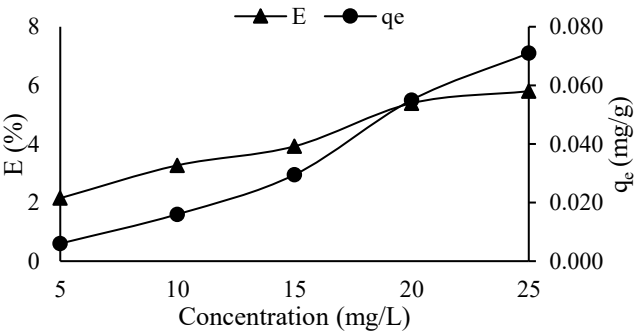

Figure 6. Relationship between removal efficiency, E (%) and adsorption capacity at equilibrium, q_e (mg/g) with different concentrations of phosphate solution

C. Adsorption Kinetics Model

Adsorption is a mechanism where solvent molecules bind to an adsorbent surface. Two major processes are involved

during an adsorption process, which are physical and chemical processes, or physisorption and chemisorption (Petrovic *et al.,* 2022). Several models are used to inspect the adsorbent's efficiency and diffusion of solutes at the surface to explain the adsorption kinetics. The pseudo-first-order (PFO) and pseudo-second-order (PSO) models are two models that have been widely used in explaining the rate of adsorption and were used in this study to analyse the data.

1. Pseudo-first-order kinetic model

PFO model, also known as the Lagergren model, assumes that the rate of change of solute uptake with time is directly proportional to the difference in saturation concentration and the amount of solid uptake with time, which is generally applicable over the initial stage of an adsorption process. It is commonly observed that the adsorption kinetics follows this PFO rate equation when adsorption occurs through diffusion through the interface (Inglezakis *et al.,* 2019). The PFO kinetic model assumes that the rate of adsorption site occupancy is proportional to the number of unoccupied sites.

In Figure 7, the general equation of a linear line is y = mx + c, where m represents gradient and c represents the y-intercept at the y-axis. Hence, by comparing the equation of PFO and the general equation of the linear line, the y-axis represents $\ln[q_e - q_t]$, c represents ln q_e, m represents $-k_1$, and x represents t (min).

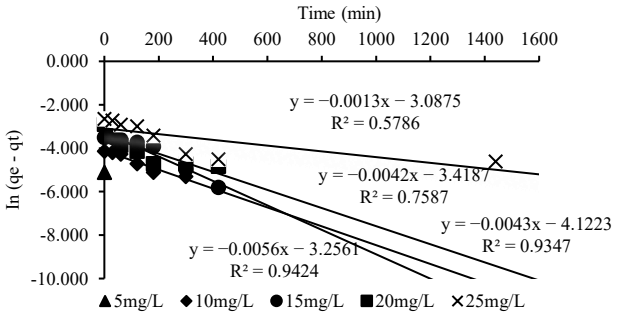

Figure 7. Linear regression analysis for PFO model for the adsorption of PO_4^{3-} onto adsorbent from a synthetic solution

Table 6 shows the kinetic parameters of PFO model which are k_1, R^2, and F_e. The most suitable kinetic model, either PFO or PSO, should have the highest correlation coefficient (R^2) and the lowest error function (F_e) value. F_e is expressed as shown in (1).

$$F_e = \sqrt{\left(\frac{1}{n-p}\right).\sum_i^n (q_t(\exp) - q_t(theo))^2} \quad (1)$$

Table 6. The kinetic parameters of PFO model

Concentrations (mg/L)	q_e (theo)	k_1	R^2	F_e	q_e (exp)
5	-	-	-	0.000	0.006
10	0.016	0.004	0.935	0.011	0.016
15	0.039	0.006	0.942	0.112	0.030
20	0.033	0.004	0.759	0.283	0.055
25	0.046	0.001	0.579	0.287	0.071

2. Pseudo-second-order kinetic model

The PSO kinetic model is a model that predicts action over the whole spectrum of adsorption, which assumes that chemical adsorption or chemisorption is the rate-limiting step. The main benefit of the PSO model compared to the PFO model is that it can be used to calculate the equilibrium adsorption capacity (Dusi *et al.,* 2022). In Figure 8, the general equation of a linear line is y = mx + c, where m represents gradient, c represents y-intercept at y-axis. Hence, by comparing the equation of PFO and the general equation of the linear line, the y-axis represents $\frac{t_i}{q_t}$, c represents $\frac{t_i}{q_e}$, m represents $\frac{1}{k_2}$, and x represents $\frac{1}{q_e^2}$. Table 7 shows the kinetic parameters of the PSO model which are k_2, R^2, and F_e. The most suitable kinetic model should have the highest correlation coefficient (R^2) and the lowest error function, F_e value.

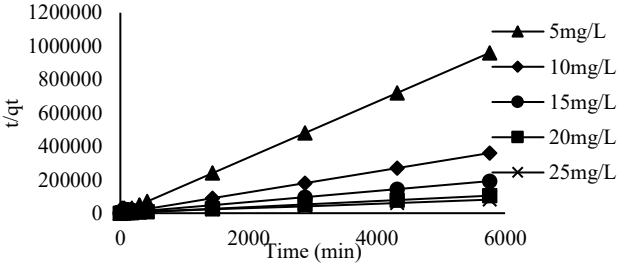

Figure 8. Linear regression analysis for PSO model for the adsorption of PO_4^{3-} onto adsorbent from a synthetic solution

Table 7. The kinetic parameters of PSO model

Concentration (mg/L)	$q_{e\ (theo)}$	k_2	R^2	F_e	$q_{e\ (exp)}$
5	0.01	0.00	1.00	2041.21	0.01
10	0.02	0.33	0.99	1.52	0.02
15	0.03	0.15	0.99	2.40	0.03
20	0.06	0.45	1.00	19.26	0.06
25	0.07	0.07	1.00	22.18	0.07

3. Comparison between PFO and PSO kinetic models

According to the results of the kinetic parameters of PSO model, the data shows that 25 mg/L concentration of aqueous solution presents the highest R^2, which is 1.00 and Fe value of 22.18. Table 8 shows the values that have been calculated for the essential parameters and correlation for the PFO and PSO models. Based on kinetic parameters obtained, the coefficient correlation of the PSO model is higher than that of the PFO model. Therefore, it can be concluded that the PSO model has a better fit for the adsorption of phosphate onto raw marsh clam shell compared to the PFO model due to the higher value of R^2. In this study, the PSO model presents a low rate of adsorption kinetics which indicates that the chemical reaction time between the adsorbent and the adsorbate to achieve adsorption equilibrium is much longer, which is at least 2880 mins. In summary, the marsh clam shell can be described to possess a large quantity of active sites which aids in PO_4^{3-} removal mechanism.

Table 8. The kinetic parameters of PFO and PSO models

PFO				
$q_{e\ (theo)}$	k_1	R^2	F_e	$q_{e\ (exp)}$
0.046	0.006	0.942	0.287	0.071
PSO				
$q_{e\ (theo)}$	k_2	R^2	F_e	$q_{e\ (exp)}$
0.07	0.45	1	22.18	0.07

D. Adsorption Isotherms Model

The main purpose of the adsorption isotherm model is to determine the condition of the adsorption whether it is monolayer or multilayer. In this study, the Freundlich model and Langmuir model were chosen for the analysis of the adsorption isotherm mechanism (Belhaj *et al.,* 2021).

1. Freundlich Model

The Freundlich isotherm model is often presented as an empirical relation between the amount of gas adsorbed by a unit mass of solid adsorbent and pressure at a specific temperature, which can explain the behaviour of adsorption (Khalil *et al.,* 2022). However, one of the weaknesses of applying the Freundlich isotherm model is that it does not illustrate the isotherms at high pressure. By referring to the linear form of Freundlich equation, $\ln q_e = \ln K_F + \frac{1}{n} \ln C_e$, the best-fit line is derived as shown in Figure 9. The graph shows the relationship between $\ln(q_e)$ and $\ln(C_e)$ for the adsorption of PO_4^{3-} onto marsh clam shell from synthetic solution, where the line increases linearly and the value of R^2 is 0.9982.

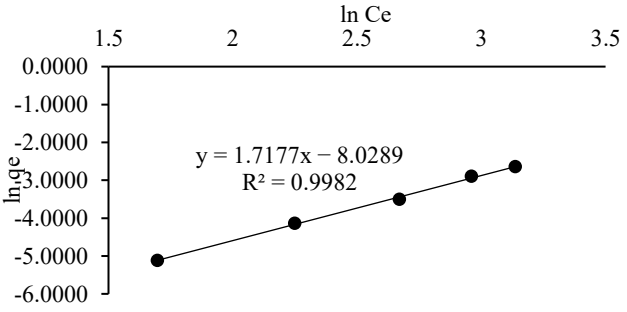

Figure 9. Linear plot of $\ln(q_e)$ versus $\ln(C_e)$ for the adsorption of PO_4^{3-} onto marsh clam shell from synthetic solution

2. Langmuir model

The Langmuir adsorption isotherm can be used to explain the equilibrium between the adsorbate and adsorbent system, where adsorption is restricted to a single molecular layer at or before a relative pressure of unity is achieved (Al-Ghouti *et al.,* 2020). By using the linear form of the Langmuir equation, $\frac{1}{q_e} = \frac{1}{K_L q_{max} C_e} + \frac{1}{q_{max}}$, the best-fit line is derived as shown in Figure 10, and the parameters q_{max}, K_L, and R^2 are identified as shown in Table 9. The R^2 value is 0.9839 which represents the coefficient of determination of the Langmuir model to identify the best fit isotherm model in describing the adsorption process of phosphate onto marsh clam shell.

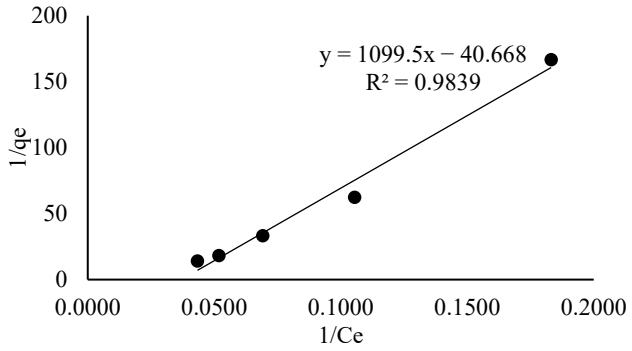

Figure 10. Linear plot of $1/q_e$ versus $1/C_e$ for the adsorption of PO_4^{3-} onto marsh clam shell from synthetic solution

3. Comparison between Freundlich model with Langmuir model

Table 9 shows the calculated values for the parameters and correlation coefficients for the Freundlich and Langmuir isotherm models. For the Freundlich model, n is the value of the heterogeneity factor, which shows a smaller value when more heterogeneous surfaces exist, and K_F is the Freundlich constant (mg/g). For the Langmuir model, q_{max} is the maximum adsorption capacity (mg/g) and K_L is the adsorption energy constant (L/mg). After comparing the correlation coefficients of the Freundlich and Langmuir models, it is clear that the experimental data is well fitted to the Freundlich model since its R^2 value is higher compared to the R^2 of the Langmuir model and is closer to 1. In summary, the adsorption in this study is a multilayer, heterogeneous process.

Table 9. Parameters for Freundlich and Langmuir isotherm models

Freundlich Model			**Langmuir Model**		
n	**K_F**	***R*²**	**q_{max}**	**K_L**	***R*²**
0.58214	0.003	0.9982	−0.0246	−0.03697	0.9839

IV. CONCLUSION

In summary, the efficiency of marsh clam shell as an adsorbent in removing phosphate from aqueous solution with various initial concentrations was investigated in this study. The highest initial concentration of aqueous solution, 25 mg/L showed the highest phosphate removal efficiency of marsh clam shell (5.80%), indicating that the rate of chemical reactions that occurred in the solution was the highest and a low concentration of phosphate was retained in the solution. In contrast, the lowest initial concentration, 5 mg/L resulted in the lowest phosphate removal efficiency, 2.15%. This indicates that removal efficiency increases when the initial concentration is increased. More phosphate ions are provided to be attached on the adsorbent surfaces, allowing the chemical reaction to occur at a fast rate and abundant phosphate ions could be eliminated in a short period.

Kinetic models and isotherm models were used to analyse the data collected in this study. The data fitted the PSO model better, which has an R^2 value of 1. Therefore, it can be known that the quantity of adsorbent is large, and the adsorption process occurs at the final stage of the reaction. For the adsorption isotherms, the data fitted better to the Freundlich model, as its correlation coefficient is higher compared to that of the Langmuir model. This indicates that the marsh clam shell contains a heterogeneous surface to allow the adsorption of phosphate, and it is a multilayer sorption. The marsh clam shell can be widely used in phosphate adsorption, as it is eco-friendly and can easily be obtained in abundance. Removing phosphate by utilising marsh clam shell also offers the added value of decreasing the dumping of marsh clam shell as well as the cost required to handle the waste products. Thus, further study is suggested to develop marsh clam shell to be used as a new green technology to extract phosphate from contaminated water sources, thus conserving the environment and helping to solve water pollution problems.

V. ACKNOWLEDGEMENT

This research was supported by Universiti Tun Hussein Onn Malaysia (UTHM) through Tier 1 (Vot J133) and Geran Penyelidikan Pascasiswazah, GPPS (Vot Q673).

VI. REFERENCES

Maksoud, MA, Elgarahy, AM, Farrell, C, Ala'a, H, Rooney, DW, & Osman, AI 2020, 'Insight on water remediation application using magnetic nanomaterials and biosorbents', Coordination Chemistry Reviews, vol. 403, p. 213096.

Abou-El-Sherbini, KS, Kenawy, IM, Hafez, MA, Lotfy, HR, & AbdElbary, ZM 2015, 'Synthesis of novel CO32−/Cl−-bearing 3 (Mg+ Zn)/ (Al+ Fe) layered double hydroxides for the removal of anionic hazards', Journal of Environmental Chemical Engineering, vol. 3, no. 4, pp. 2707-2721.

Alabbad, EA, Bashir, S, & Liu, JL 2022, 'Efficient removal of direct yellow dye using chitosan crosslinked isovanillin derivative biopolymer utilizing triboelectric energy produced from homogeneous catalysis', Catalysis Today, vol. 400, pp. 132-145.

Al-Ghouti, MA & Da'ana, D A 2020, 'Guidelines for the use and interpretation of adsorption isotherm models: A review', Journal of Hazardous Materials, vol. 393, pp. 122383.

Belhaj, AF, Elraies, KA, Alnarabiji, MS, Kareem, FAA, Shuhli, JA, Mahmood, SM & Belhaj, H 2021, 'Experimental investigation, binary modelling and artificial neural network prediction of surfactant adsorption for enhanced oil recovery application', Chemical Engineering Journal, vol. 406, pp. 127081.

Dehvari, K, Chiu, SH, Lin, JS, Girma, WM, Ling, YC & Chang, JY 2020, 'Heteroatom doped carbon dots with nanoenzyme like properties as theragnostic platforms for free radical scavenging, imaging, and chemotherapy', Acta Biomaterialia, vol. 114, pp. 343-357.

Dodd, MS, Zhang, Z, Li, C, Algeo, TJ, Lyons, TW, Hardisty, DS & Wang, W 2021, 'Development of carbonate-associated phosphate (CAP) as a proxy for reconstructing ancient ocean phosphate levels', Geochimica et Cosmochimica Acta, vol. 301, pp. 48-69.

Dusi, GG, Marques, GS, Kienteca, ML, Gimenes, ML, Cerutti, MLMN & da Silva, VR 2022, 'Biosorption investigation of Cu (II) ions from aqueous solutions using sericin–alginate particles: Kinetic, equilibrium, and thermodynamic,' Sustainable Chemistry and Pharmacy, vol. 25, p. 100601.

El-Khaiary, MI, Malash, GF, & Ho, YS 2010, 'On the use of linearized pseudo-second-order kinetic equations for modelling adsorption systems', Desalination, vol. 257, no. 1-3, pp. 93-101.

Gong, XL, Lu, HQ, Li, K, & Li, W 2022, 'Effective adsorption of crystal violet dye on sugarcane bagasse–bentonite/sodium alginate composite aerogel: Characterisation, experiments, and advanced modelling', Separation and Purification Technology, vol. 286, p. 120478.

Hairom, NHH, Soon, CF, Mohamed, RMSR, Morsin, M, Zainal, N, Nayan, N & Harun, NH 2021, 'A review of nanotechnological applications to detect and control surface water pollution', Environmental Technology & Innovation, vol. 24, p. 102032.

Inglezakis, VJ, Fyrillas, MM, & Park, J 2019, 'Variable diffusivity homogeneous surface diffusion model and analysis of merits and fallacies of simplified adsorption kinetics equations', Journal of Hazardous Materials, vol. 367, pp. 224-245.

Kasim, NZ, Abd Malek, NAA, Anuwar, NSH, & Hamid, NH 2020, 'Adsorptive removal of phosphate from aqueous solution using waste chicken bone and waste cockle shell', Materials Today: Proceedings, vol. 31, pp. A1-A5.

Khalil, KM, Elhamdy, WA, & Elsamahy, AA 2022, 'Biomass derived P– doped activated carbon as nanostructured mesoporous adsorbent for chromium (VI) pollutants with pronounced functional efficiency and recyclability', Colloids and Surfaces A: Physicochemical and Engineering Aspects, vol. 641, p. 128553.

Khamwichit, A, Dechapanya, W & Dechapanya, W 2022, 'Adsorption kinetics and isotherms of binary metal ion aqueous solution using untreated venus shell', Heliyon, vol. 8, no. 6.

Kończyk, J, Kluziak, K, & Kołodyńska, D 2022, 'Adsorption of vanadium (V) ions from the aqueous solutions on different biomass-derived biochar's', Journal of Environmental Management, vol. 313, p. 114958.

Koohsaryan, E, Anbia, M & Maghsoodlu, M 2020, 'Application of zeolites as non-phosphate detergent builders: A review', Journal of Environmental Chemical Engineering, vol. 8, no. 5, p. 104287.

Mohammed, AA & Kareem, SL 2019, 'Adsorption of tetracycline from wastewater by using Pistachio shell coated with ZnO nanoparticles: Equilibrium, kinetic and

isotherm studies', Alexandria Engineering Journal, vol. 58, no. 3, pp. 917-928.

Petrovic, B, Gorbounov, M & Soltani, SM 2022, 'Impact of surface functional groups and their introduction methods on the mechanisms of CO2 adsorption on porous carbonaceous adsorbents', Carbon Capture Science & Technology, vol. 3, p. 100045.

Prihanto, A, Fitriyana, DF, Muryanto, S, Masykur, I, Ismail, R, Jamari, J & Bayuseno, AP 2021, 'Aqueous crystallization of monocalcium phosphate monohydrate with green mussel shells (*Verna piridis*) for calcium sources', Journal of Environmental Chemical Engineering, vol. 9, no. 6, p. 106913.

Qu, G, Zhou, J, Liang, S, Li, Y, Ning, P, Pan, K & Tang, H 2022, 'Thiol-functionalized multi-walled carbon nanotubes for effective removal of Pb (II) from aqueous solutions', Materials Chemistry and Physics, vol. 278, p. 125688.

Rashid, SS, Liu, YQ & Zhang, C 2020, 'Upgrading a large and centralized municipal wastewater treatment plant with sequencing batch reactor technology for integrated nutrient removal and phosphorus recovery: Environmental and economic life cycle performance', Science of the Total Environment, vol. 749, p. 141465.

Schweitzer, L & Noblet, J 2018, 'Water contamination and pollution', in Green chemistry, pp. 261-290.

Kumar, PS, Suganya, S, Srinivas, S, Priyadharshini, S, Karthika, M, Karishma Sri, R & Lichtfouse, E 2019, 'Treatment of fluoride-contaminated water: A review', Environmental Chemistry Letters, vol. 17, pp. 1707-1726.

Sharma, P, Tripathi, S, Vadakedath, N & Chandra, R 2021, 'In-situ toxicity assessment of pulp and paper industry wastewater on *Trigonella foenum-graecum* L: Potential source of cytotoxicity and chromosomal damage', Environmental Technology & Innovation, vol. 21, p. 101251.

Solangi, NH, Kumar, J, Mazari, SA, Ahmed, S, Fatima, N & Mubarak, NM 2021, 'Development of fruit waste derived bio-adsorbents for wastewater treatment: A review,' Journal of Hazardous Materials, vol. 416, p. 125848.

Steigerwald, JM & Ray, JR 2021, 'Adsorption behaviour of perfluorooctanesulfonate (PFOS) onto activated spent coffee grounds biochar in synthetic wastewater effluent', Journal of Hazardous Materials Letters, vol. 2, p. 100025.

Wang, R, Wang, Q, Dong, L & Zhang, J 2021, 'Cleaner agricultural production in drinking-water source areas for the control of non-point source pollution in China', Journal of Environmental Management, vol. 285, p. 112096.

Woo, SY, Lee, HS, Kim, JS, Kim, KH, Ji, H & Kim, YD 2022, 'Applicability assessment of functional adsorption zeolite materials in adsorption desalination cum cooling systems driven by low-grade heat source', Chemical Engineering Journal, vol. 430, p. 131375.

Yukhajon, P, Somboon, T & Sansuk, S 2023, 'Enhanced adsorption and colorimetric detection of tetracycline antibiotics by using functional phosphate/carbonate composite with nanoporous network coverage', Journal of Environmental Sciences, vol. 126, pp. 365-377.

Zhang, J, Chen, L, Yin, H, Jin, S, Liu, F & Chen, H 2017, 'Mechanism study of humic acid functional groups for Cr (VI) retention: two-dimensional FTIR and 13C CP/MAS NMR correlation spectroscopic analysis', Environmental Pollution, vol. 225, pp. 86-92.

Zhang, J, Tian, Z & Wang, K 2020, 'Study on the defect of sulphur substituting for phosphorus in potassium dihydrogen phosphate', Chinese Journal of Physics, vol. 67, pp. 86-90.